

DEVELOPMENT OF COMBINED ORGANOSOLV-TEMPO OXIDATION TREATMENT FOR OBTAINING CELLULOSE NANOFIBRES

PABLO LIGERO,* ALBERTO DE VEGA* and XOAN GARCÍA**

**Universidade da Coruña, Bio-Based Products Group (BBP),
Centro de Investigacións Científicas Avanzadas (CICA), Campus de Elviña, 15071 A Coruña, Spain*
***Intasa Group, Research Department, A Braña, s/n, 15147 Coristanco, A Coruña, Spain*
✉ *Corresponding author: P. Ligeró, pablo.ligeró@udc.gal*

Received December 27, 2022

The aim of this work was to study and optimize the production of nano-size cellulose fibrils (NFC) by combined performic acid treatment, totally chlorine-free (TCF) bleaching and TEMPO-oxidation prior to mechanical treatment. For this purpose, a face-centered design was developed in order to optimize the independent variables governing performic treatment. Under the optimal conditions, a kappa index of 13 was achieved, which decreased to 2.2 after bleaching treatment. These low-lignin pulps were TEMPO-oxidized under different oxidizing conditions, while monitoring cellulose yield, carboxylic acid content and the degree of polymerization. The optimized conditions produced oxidized pulp with 1.4 mmol COOH/g dried nanofibre. Finally, this oxidized cellulose was subjected to high-pressure mechanical processing in order to obtain cellulose nanofibres. From the results, it can be concluded that neither the number of homogenizer passes nor the pressure affected to diameter of fibrils.

Keywords: organosolv fractionation, performic acid delignification, alkaline TEMPO-oxidation and nanofibers of cellulose

INTRODUCTION

Cellulose is used mainly to produce paper; however, the demand of new cellulose-based products is growing. Among these products, cellulose fibres with diameters of a few nanometres, named nanofibers,¹ are under study among researchers. This material is a potential valuable product due to its ability to reinforce other structures, such as paper, composites, resins *etc.*²⁻⁴ However, nano-sized cellulosic fibres must be “released” from a biomass matrix. For this, different methods have been proposed, from mechanical to chemical ones. Chemical methods use a combination of pulping and bleaching operations, aiming at the production of highly pure cellulose before its disintegration. For this purpose, the use of low environmental impact pulp production systems has been investigated by several researchers as an alternative to traditional sulphur methods. Among them, the organosolv process is called like this as it uses an organic solvent as fractionation agent. A great variety of organic solvents that have been tested for chemical pulping can be found in the literature.⁵⁻⁹ Among them, the Milox process consists of a

two-step peroxide-formic treatment.^{10,11} In the first phase, lignin is attacked by OH⁺ ions, which come from the *in-situ* reaction between the carboxylic acid and hydrogen peroxide. In the second stage, the main delignification happens by hydrolysis of beta-aryl ethers. Even so, depending on the raw materials and the objective sought, the process has been applied to some materials in a single stage,^{12,13} in two stages^{14,15} or as a three-stage peroxyformic treatment.¹⁶

The aim of this work was to test the ability of the peroxyformic method to produce cellulose pulp from *Pinus* spp. with enough quality to yield nanocellulose. The effect of the variables on the delignification progress was quantified and modelled by a factorial experimental design. Later, the pulp obtained under the best conditions of delignification was subjected to the TCF bleaching sequence (EPab) to produce suitable pulp for nanocellulose production.

Eventually, the high purity cellulose produced was subjected to chemical oxidation prior to mechanical treatment. The aim of the chemical oxidation was to increase the content of

carboxylate groups to facilitate the subsequent separation of fibres by mechanical treatment. The influencing variables on the process were quantified and modelled by a face-centred experimental design to achieve the optimal oxidation conditions based on the carboxyl content.

EXPERIMENTAL

Raw material

Pinus spp. samples originated from the Atlantic forest in the Northwest of Iberian Peninsula. Samples were milled and the fraction that passed through 1 mm sieve (less than 1 mm particle size) was selected. Milled samples were air-dried until they reached equilibrium moisture and kept in hermetic bag until use.

Kappa number, Klason lignin (KL) content, ash, extractives and intrinsic viscosity were measured according to Tappi standards (T236, T22-om88, T211-om02, T204-cm97 and T230, respectively). Pulp yield (PY) was measured gravimetrically after samples had been dried until constant weight. Cellulose was determined according to the method described by Bauer and Ibáñez.¹⁷

Monosaccharides were measured by liquid chromatography in a HPLC equipped with an RI detector and an Aminex HPX-87H column (BIORAD, California, USA).

The carboxyl content of oxidized cellulose was determined by conductometric titration with NaOH. Dried samples (100 mg) were suspended in 0.01M HCl until pH 2.5-3 was attained, to ensure the exchange of Na ions by H ions in COOH groups. Then, the acidic samples were titrated against 0.05M NaOH, registering conductivity against the volume of alkali added. The conductometric titration showed the presence of a strong acid corresponding to excess to the HCl excess and a weak acid corresponding to the carboxyl acid. The carboxyl concentration was calculated with the following equation in mmol/g dried oxidized cellulose:

$$CC(\text{mmol/g dried oxidized fibres}) = \frac{(V_1 - V_2) \cdot c}{w} \quad (1)$$

where V_1 and V_2 are the volumes in mL of 0.05N NaOH added, corresponding to the final strong acid neutralization and final weak acid neutralization, respectively.

Microscopy observations

The diameter of the fibres was determined using a transmission electronic microscope (TEM). The technique followed consisted of depositing the sample on a carbon film grid and negative staining with 2% uranyl acetate in water for 30 min. The treated samples were observed in a TEM JEOL JEM-2011 at 90 KV.

Structural analysis of samples

Fourier-transform infrared spectroscopy of initial pulp, bleached pulp and nanocellulose was performed in the Attenuated Total Reflectance (ATR) mode. For this, a Bruker Vector 22 mid-infrared FTIR spectrometer, equipped with a single-reflection diamond ATR accessory (model Golden Gate, Specac) was used. All spectra were acquired at ambient temperature in the range of 400-4000 cm^{-1} (64 scans).

The structures of initial pulp, bleached pulp and nanocellulose were analysed by a Siemens D5000 X-ray diffractometer. The analysis was performed at a scanning speed of 0.02°/min from $2\theta = 5$ to 50° with Cu-K α radiation ($\lambda = 1.54 \text{ \AA}$, $V = 40\text{kV}_{\text{accelerating}}$ and $I = 30 \text{ mA}$). Crystallinity index was determined by the method of Segal *et al.*:¹⁸

$$C_r I(\%) = \frac{(I_{200} - I_{am})}{I_{200}} \cdot 100 \quad (2)$$

where I_{200} is the maximum intensity of the 200 reflection plane attributed to the crystalline domain and I_{am} corresponding to the amorphous zone of cellulose. The thermal stability was determined on a Netzsch STA 449F3 thermal analyser, under nitrogen atmosphere, at a heating rate of 5 °C/min from 20 °C to 600 °C.

Pulping treatment

The raw material was subjected to two-step peroxyformic treatment at different formic acid concentrations, hydrogen peroxide content and temperature conditions, with 12/1 liquid/wood ratio, for 60 minutes. In the first phase, samples were subjected to peroxyformic delignification. For this, 2 g of air-dried sample and a solution of the chosen formic acid concentration (FAC) were heated in a 100 mL round-bottom flask until the chosen temperature was reached. At this moment, a desired amount of hydrogen peroxide (HPC) was added, taking this time as initial. After the treatment, the pulp was filtered and washed three times with 85% formic acid and neutralised with distilled water. In the second step, the pulp from the optimised peroxyformic process was delignified with boiling concentrated formic acid during the chosen time. The pulp was then filtered and washed with 85% formic acid. Eventually, samples were soaked with distilled water until neutrality.

Bleaching

The TFC bleaching treatment was optimised for organosolv pulps of pine pulp,¹⁹ which consisted of an EPab sequence, namely, an alkaline step (E) and a peracetic step at pH 11 (Pab). Bleaching experiments were carried out at 10% consistency in sealed polyethylene bags immersed into a thermostatic water bath at the desired temperature for one hour, 70 °C and 60 °C for alkaline and peracetic process, respectively.

The pulp from the alkaline treatment was soaked with an aqueous solution at pH 11 before the

peroxiacetic process. After the treatment, samples were filtered and washed three times with an aqueous solution at pH 11 and neutralised with distilled water.

Nanofibre production

The bleached pulp was oxidised by the TEMPO-catalysis before mechanical homogenization. For this, the pulp was suspended in 1% aqueous solution at pH 10, then the TEMPO reagent (1.6% dried pulp basis) and NaBr (1% dried pulp basis) were added. The suspension was heated until the chosen temperature, then a 15% NaClO solution was added to get the desired concentration for each experiment. The pH was maintained at the value of 10 by the addition of 0.5 M NaOH solution. After oxidation, the samples were filtered and washed with distilled water. An aqueous suspension of 1% oxidised pulp was homogenised in a high-pressure lab homogenizer Panda PLUS 2000 (GEA NIRO, Parma, Italy) at different pressures and number of passes through the homogenizer.

RESULTS AND DISCUSSION

The raw material was supplied by a middle-size board manufacturing plant. The raw wood was characterized in terms of its chemical composition.

Table 1 shows the average values and standard deviations for the contents of the main components of the samples used in this work. The raw material presented a high lignin content, as shown by the Klason lignin value (KRL) (29%), this value being in agreement with those reported by Mattos et al.²⁰ and Cruz et al.²¹ for pine wood and *Pinus radiata*, respectively. The same situation is extensible to cellulose, but the hemicelluloses content lies between the data described in the cited works (15.6%). Xylose is the main component in hemicelluloses, accounting for 95%. The content of extractives was slightly higher than that found by Mattos et al.²⁰ (8.2% on dried raw material basis). Finally, it should be noted that the *Pinus* spp. used in this work presents very low ashes content.

Two-step performic pulping

Table 2 shows the structure of the experimental design, together with the results obtained in each case for pulp yield (PY), residual Klason lignin (KL) in pulp, viscosity and kappa index of pulp.

Table 1
Chemical characterization of pine wood

Parameter	Value	Standard dev.
KRL	29.4	0.8
Cellulose	35.7	4.9
Hemicelluloses	20.8	4.4
Xylose	18.7	3.3
Extracts	10.4	0.9
Ash	0.3	0.1

Table 2
Experimental design of pulping process

FAC	HPC	Temp.	PY	LKR	Dis. cellulose	Kappa	Viscosity,
% in liquor		°C	% dried pulp				mL/g
75	2	60-80	88.5	14.6	-3.1	61.7	344.1
75	2	80	75.5	16.3	0.7	53.3	302.7
75	5	60	80.3	2.2	0.2	20.8	421.0
75	5	80	80.9	1.3	-0.6	6.1	292.3
82	2	60	85.0	13.9	4.2	50.1	387.3
82	2	80	77.3	13.1	5.2	51.4	302.8
82	5	60	76.0	1.1	-2.4	17.3	355.5
82	5	80	98.1	2.7	12.1	6.2	303.0
78.5	3.5	70	78.9	3.1	-1.2	18.6	364.3
78.5	3.5	70	107.7	2.1	-2.2	19.7	353.8
78.5	3.5	70	87.6	4.0	1.6	28.6	367.8
75	3.5	70	96.8	3.2	4.8	24.3	357.9
82	3.5	70	111.6	0.3	-8.9	15.6	410.1
78.5	2	70	101.0	10.5	1.2	45.3	361.0
78.5	5	70	115.7	2.4	-2.2	8.8	344.4
78.5	3.5	60	109.6	3.3	2.1	32.9	384.5
78.5	3.5	80	102.7	1.8	4.3	13.8	355.3

Table 3
Regression parameters for each variable, as well as goodness of fit and significance of regression equations

Factor	PY	Kappa	LKR	Viscosity	Cellulose dissolved
b ₀	53.40	20.58	2.29	371.91	54.97
b ₁ (FAC)	-0.84	-2.56	-0.64	4.05	-0.65
b ₂ (HPC)	-6.69	-20.26	-5.88	1.83	5.83
b ₃ (Temperature)	-4.36	-5,198	0.018	-33.64	-0.30
R ²	0.96	0.9720	0.9645	0.8566	0.5913
Adj. R ²	0.8873	0.9255	0.9055	0.6176	-0.0898
F	13.5971	20.8652	16.3232	3.5842	0.8681
Sig. F	0.0023	0.0007	0.0014	0.0659	0.5989

The fitting of the experimental results by means of least square multiple regression provided the results presented in Table 3, which shows the different parameters of the model, their significance levels, and several statistical values that indicate the goodness of fit of the mathematical models.

The results show a good adjustment between the experimental data and the predicted values, except for viscosity, as indicated by the values of R² and F (Table 3).

For kappa index, the model shows good statistical parameters for prediction and goodness of fit (Table 3).

The hydrogen peroxide percentage in liquor is the most significant independent variable in the delignification process, followed by the temperature. The peroxide influence is much more significant than that of the temperature, as shown in the fitting parameters. Moreover, the coefficients of regression are negative in both cases, meaning that the lignin content decreases as the peroxide percentage and temperature increase. Figure 1 shows the kappa index *versus* hydrogen peroxide percentage and temperature at fixed formic acid content. In this graph, the difference between chemical and thermal influence can be clearly appreciated. A pronounced descendent slope is observed when peroxide concentration increases, reaching a value as low as 6 at 80 °C. The kappa index drop is moderate when temperature increases, thus no significant reduction is observed beyond 70 °C.

The lowest values of the kappa index (6.1-6.2) were obtained at maximum hydrogen peroxide percentage (5.0%) with temperature over 70 °C, regardless of the formic acid percentage. Despite this value being very low, it should be pointed out that it was obtained at the expense of an important solubilisation of materials and pulp damage, as evidenced by the low pulp yield (less than 50%), high cellulose dissolution (around 12%) and low

viscosity (around 300 mL·g⁻¹). However, in general, the delignification process was very selective, as shown in Figure 2, where it can be observed that a high ratio of mass losses corresponds to lignin dissolution, except under the harsh conditions mentioned. This is confirmed by the viscosity values that were not altered much by delignification, except when the lignin removal was high (at the lowest kappa values), the viscosity drop was bigger.

The viscosity model, despite having a low value of R² (Table 3), presented an interesting characteristic: it only significantly depended on temperature. The correspondent coefficient value was high and negative; therefore, a slight temperature rise caused a pronounced drop in viscosity values. On the other hand, the maximum viscosity was reached at a low temperature, regardless of peroxide percentage. Nevertheless, all other first-order parameters were negative, indicating loss in viscosity when FAC, HPC and temperature rose. These facts are reflected in Figure 3, where the variations in viscosity can be observed depending on the temperature and the peroxide, for fixed values of formic acid concentrations. The yield model shows a similar trend to the one of the kappa index. Hydrogen peroxide percentage and temperature are highly significant variables, being the first more important quantitatively. Moreover, the regression coefficients were negative, meaning that its value diminished as all values of independent variables increased. This fact was more pronounced for peroxide content in the reaction medium, reflected in a bigger slope along the axis, as shown in Figure 4. The minimum yield was obtained for a maximum peroxide concentration, reaching a value below 50%.

The difference between the viscosity behavior and pulp yield can be attributed to a higher contribution of acid hydrolysis as temperature increases, which causes a reduction of cellulose

length at the higher temperature assayed. Later, the model for dissolved cellulose was also calculated, but its regression was not good, as the low R^2 value

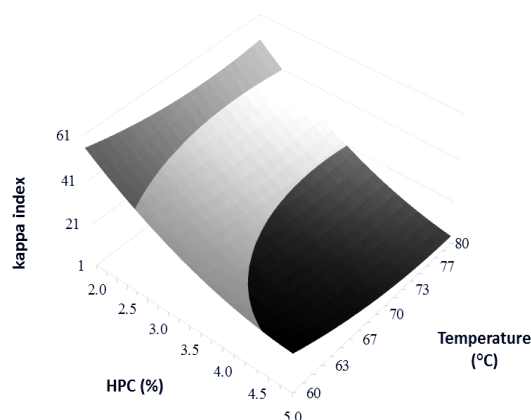


Figure 1: Effect of hydrogen peroxide and temperature variations on kappa index

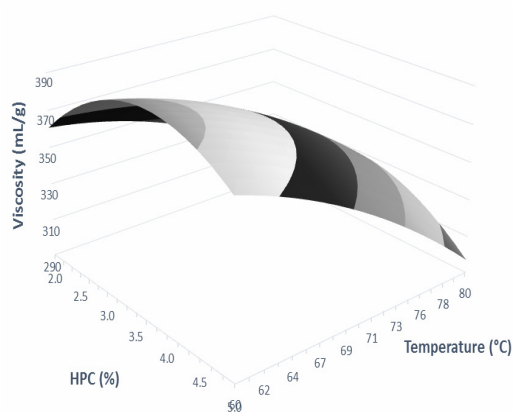


Figure 3: Viscosity variations at different temperature and hydrogen peroxide content (HPC)

Optimization of the pulping process

Finally, an optimization criterion was established in order to obtain the highest delignification of pulp, by the mathematical optimization of the regression equations obtained, with the following simultaneous conditions and their weights in the algorithm: pulp yield $\geq 55\%$ = (55%), dissolved cellulose: $\leq 5\%$ (10%), viscosity ≥ 400 mL/g = (5%) and index kappa ≤ 23 = (30%). The results of the optimized model are presented in Table 4. The fractionation under these conditions became very good, namely: 88% delignification, 82% hemicellulose solubilisation, and only 6% dissolved cellulose.

Samples from optimized performic acid pulping were subjected to boiling formic acid

shows (Table 3), meaning no independent variable influences the dissolved cellulose for a 95% confidence interval.

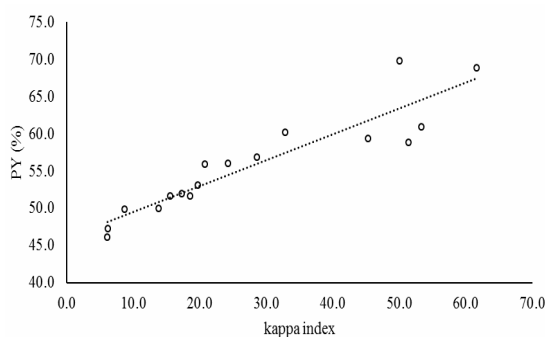


Figure 2: Kappa index versus pulp yield in performic acid treatment

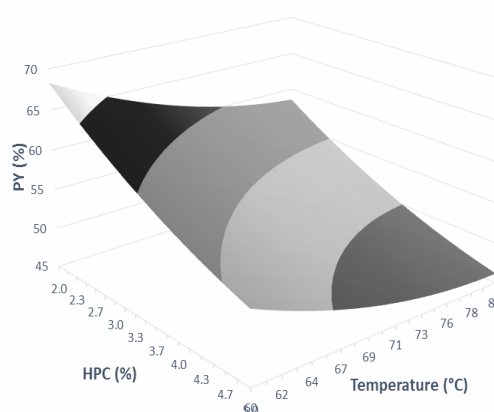


Figure 4: Pulp yield variations at different temperature and hydrogen peroxide content (HPC)

treatment at different times (5, 15 and 60 minutes). The results showed that the shortest time was enough to get a good quality low-lignin pulp, reaching a kappa index of 13, 1.6% of dissolved cellulose and 46.2% of pulp yield.

Bleaching of organosolv pulp

To continue the delignification, two TCF treatments were assayed, namely: alkaline extraction (E-stage) and peracetic acid (Pa-stage) at alkaline pH. As the pulp obtained from the two-step performic acid treatment had low lignin content, the decision was made to apply a short TFG treatment at conditions previously optimized with other species (Table 5). The result of the bleaching process was a low-lignin pulp,

reaching values of 2.2 in kappa index and 333 mL/g for viscosity with only 2% of dissolved material.

Preparation of cellulose nanofibres

Pulp produced from performic acid pulping and TCF bleaching was ready to be oxidized by TEMPO, prior to mechanical treatment. For this, bleached pine wood pulp was subjected to TEMPO-catalytic oxidation at pH 10. Different assays were developed, in which, three independent variables: oxidizing agent (NaClO) content, temperature and time were modified in order to study their relation to the carboxylic acid produced, yield of oxidized cellulose and polymerization degree.

Table 6 shows the assays performance, together with the carboxylic groups produced, yield of nanofibres and polymerization degree. As expected, the carboxylate groups content increased as NaClO rose for a similar amount of catalyst. In fact, the oxidizing reagent concentration was the most significant variable in COO⁻ production. In Figure 5, the carboxylic group concentration vs NaClO and operation time is shown. A fast growth of carboxylic groups on the surface of fibres can be observed when the oxidizing agent amount is raised from 3 to 8 mmol/g, after that, a decreasing trend starts under harsher conditions. This effect was likely caused by oxidation of C2-C3 predominantly at pH 11.²²

Table 4
Optimized variables from experimental design

Variable	Value
HCOOH (% by weight in reaction liquor)	82
H ₂ O ₂ (% by weight in reaction liquor)	3.9
Temperature 1 st stage (°C)	60
Time 2 nd (minutes)	5

Table 5
Bleaching conditions

Stage	NaOH Weight % in liquor	CH ₃ COOOH % in liquor	pH	Temperature, °C	Time, min	PY (%)	Kappa index	Viscosity, mL/g
E	6	-	-	70	60	96.8	-	-
Pab	-	7	10	55	60	99.1	2.2	333

Table 6
Experimental conditions and results of TEMPO-oxidation

NaClO, mmol/g d.p.b.	Temp., °C	Time, min	COOH, mmol/g d.p.b.	Int. viscosity (mL/g)	PY, %
2.5	25	30	0.27	159.9	88.5
2.5	25	300	0.57	142.5	75.5
2.5	50	30	0.25	152.4	80.3
2.5	50	300	0.42	133.4	80.9
12	25	30	0.61	122.5	85.0
12	25	300	1.10	114.3	77.3
12	50	30	0.75	107.5	76.0
12	50	300	0.53	91.5	98.1
7.25	37.5	165	0.73	90.5	78.9
7.25	37.5	165	0.63	89.8	107.7
7.25	37.5	165	0.51	90.9	87.6
2.5	37.5	165	0.31	165.4	96.8
12	37.5	165	1.46	73.7	111.6
7.25	25	165	1.42	76.3	101.0
7.25	50	165	1.35	73.1	115.7
7.25	37.5	30	1.27	89.1	109.6
7.25	37.5	300	0.94	91.2	102.7

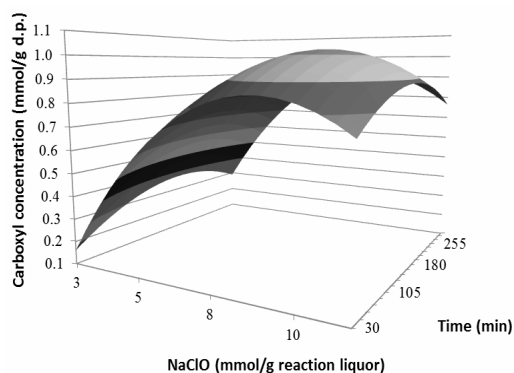


Figure 5: Effect of NaClO content and reaction time on carboxyl formation

From the results shown in Table 6, it can be concluded that time was an important factor only when samples were treated under the softest conditions. At the lowest values of NaClO concentration and temperature, the carboxyl amount was doubled when the time was raised from 30 to 300 minutes. Moreover, under mild oxidation conditions, the value of COOH in the bleached pulp was always the lowest of the assays tested.

Eventually, the results showed that temperature had no influence on the production of COO⁻ groups. Thus, in this situation, an increase in temperature affected the carboxyl content only in the bottom range of reaction conditions, as observed in Table 6. On the other hand, the carboxyl content obtained was similar to that described by Serra *et al.*,²³ when the amount of catalyst in TEMPO-oxidation was studied for bleached eucalyptus pulp.

The intrinsic viscosity shows a similar trend to that of the carboxyl group production, since NaClO concentration was the most influential independent variable towards viscosity values (Fig. 6). In fact, its regression parameter was 4 times higher than those for time and temperature. This coefficient was negative, meaning a decrease in viscosity as NaClO increased, registering a reduction close to 50% under harsh oxidation conditions. This result corresponded to those reported by Masuki *et al.*,²² when they studied nanocellulose production by NaClO-oxidation prior to the mechanical process. The authors attributed the loss of the original structure of fiber to depolymerization caused by NaClO oxidation.

This effect was also observed by Besbes *et al.*,²⁴ when the effect of the carboxyl content on the high-pressure defibrillation of oxidized eucalyptus

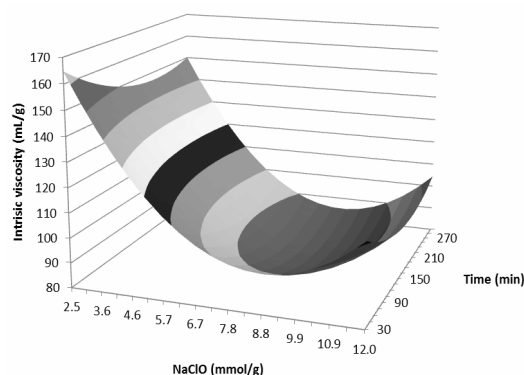


Figure 6: Effect of NaClO and time variations on intrinsic viscosity

pulp was studied. Electrostatic repulsion between carboxylate groups on the surface of the nanofibres reduced the strength of bonds among NFC, resulting in a lower viscosity of the suspension. This effect can explain why the drop of viscosity was not followed by the pulp yield decrease when carboxyl groups were increasing (Fig. 7). Serra *et al.*²³ attributed this effect to the degradation of cellulose at alkaline pH, although, in this case, no significant losses of cellulose were observed.

Finally, in order to obtain the best results via TEMPO-mediated oxidation, a mathematical optimization was performed. The following simultaneous conditions and their weights in the algorithm were used: carboxyl content: ≥ 1.4 mmol/g dried nanofibre (35%), minimum nanofibre yield (50%), intrinsic viscosity ≥ 200 (15%). From this optimization, the following oxidation conditions were obtained: 9 mmol NaClO/g dried raw material, temperature of 25 °C and 220 minutes of reaction time. Under these conditions, the model predicted 1.4 mmol COOH/g dried nanofibres, nanofibre yield of 98% and viscosity of 125 mL/g.

The last step of this work was to study the relation between the diameter of nanofibres and the number of passes through the homogenizer. For this, the suspension of oxidized fibre was dispersed in water at a fibre content of 1 wt% and then homogenized by passing through a high-pressure homogenizer, operating at a pressure ranging from 300 to 800 bar, for a different number of times. The conditions tested, together with the results for fibre diameter and viscosity of the nanofibre suspension, are described in Table 7.

The results indicated that the diameter distribution was similar for all the conditions investigated. In fact, the diameter was only

reduced slightly when the number of passes increased from 3 to 5 at lower pressure (300 and 500 bar). Furthermore, from the results shown in Table 7, an increase in the suspension viscosity was observed as the number of passes increased. This effect can be attributed to the enhanced effect of homogenisation on fibrillation, causing a stronger network structure.

For a deeper insight into the morphology of nanofibres, TEM observations were carried out (Fig. 8). For this, 1 wt% nanofibre suspensions were studied under electronic microscopy. Observations revealed that all samples presented nano-sized network fibril structures, with widths varying between 4.5-2.2 nm. This range of diameters showed that fibrillation was effective, and no fibre fragments were found. Moreover, from the diameter results, it can be concluded that the pressure has no influence on the fibre diameter.

Finally, the images of nanofibres were compared with those of unbleached and bleached pulp (Fig. 8). It was observed that the diameter decreased throughout chemical treatment, being

reduced from around ten microns to half of its value. Also, it was observed that the fibre structure suffered a collapse caused by the chemical delignification.

Analysis of samples throughout nanocellulose production

ATR-FTIR analysis

All samples from different treatments were analysed by ATR-FTIR spectroscopy to identify the main functional groups. The FTIR ATR spectra in absorbance terms are shown in Figure 9.

In all cases, a broad band was observed in the 3500-3000 cm^{-1} region, which was attributed to aliphatic and aromatic O-H stretching vibrations. This band had higher intensity in the bleached sample, which likely corresponds to the OH groups introduced by the peroxyacetic molecule. A similar effect was reported by Robles *et al.*,²⁵ for organosolv pulp of blue agave bleached with peroxide. The band at 3000-2800 cm^{-1} corresponded to symmetrical and asymmetrical C-H stretching of CH_2 groups of cellulose.

Table 7
Diameter, viscosity and density of nanofibres after homogenization

Sample	Pressure, bar	Number of passes	Intrinsic viscosity, mL/g	Diameter, nm	Density, g/mL
3001	300	1	38.9	3-4.5	0.99
3005	300	5	47.2	2.8-3.1	0.82
5001	500	1	83.6	2.9-4.0	1.07
5005	500	5	89.2	2.8-4.9	0.98
30036001	300/600	3/1	139.0	3.1-4.0	1.00
30036005	300/600	3/5	104.2	3.7-4.8	1.05
300360010	300/600	3/10	89.7	2.2-3.7	0.98
300580010	300/800	5/10	86.7	2.5-4.8	0.98
500580020	500/800	5/20	85.2	2.2-3.7	0.97

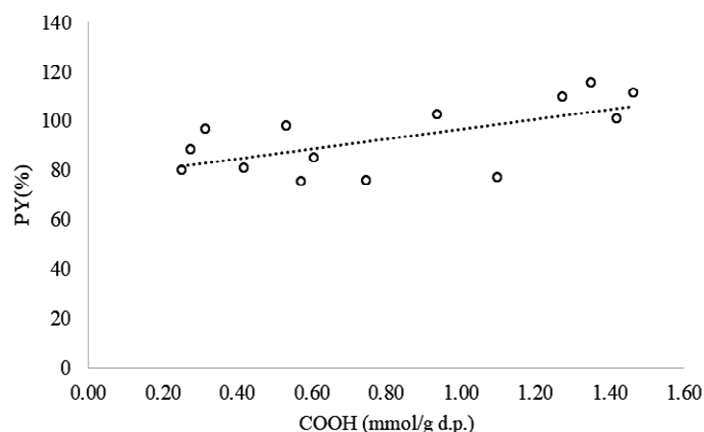


Figure 7: Relationship between PY and concentration of carboxyl groups

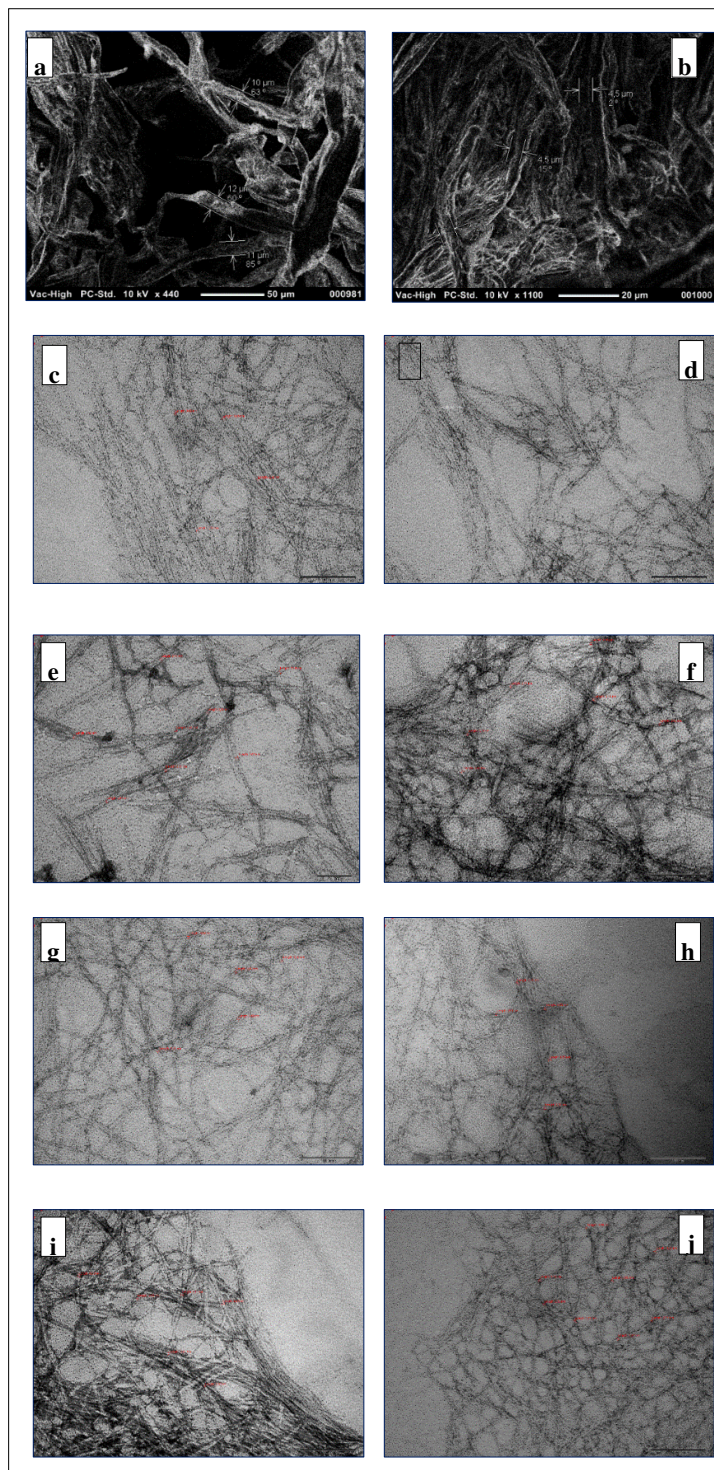


Figure 8: TEM images of a) delignified pulp; b) bleached delignified pulp; as well nanofibre samples c) 3001; d) 3005; e) 5001; f) 5005; g) 30036001; h) 30036005; i) 3003080010 and j) 500580020

The band around 1720 cm^{-1} can be attributed to the carbonyl group of hemicelluloses. In organosolv pulp, the intensity was higher than in alkaline, which corresponds to a higher content of

hemicelluloses in the first case. Moreover, this signal disappeared in the spectra of nanocellulose, as expected. After peroxide delignification,

samples showed an increase in this region due to the oxidation of cellulose aldehyde groups.

On the other hand, the signal at 1600 cm^{-1} present in the spectrum of nanocellulose, corresponding to the sodium carboxylate group,²⁶ was consistent with a higher amount of COONa

groups incorporated during the TEMPO-oxidation process at basic pH.

The band at $1050\text{--}1025\text{ cm}^{-1}$ can be related to C-O-C stretching vibrations of glucose in pyranose form and at 897 cm^{-1} corresponding to cellulosic β -glycosidic linkage.

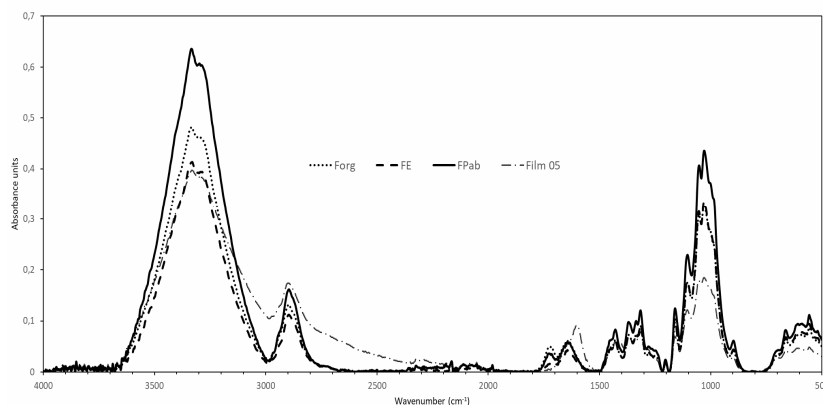


Figure 9: FTIR-ATR spectra of organosolv pulp (Forg), pulp after alkaline process (FE), bleached pulp (FEPab) and nanocellulose obtained after 5 homogenizer passes (Film 05)

Thermal analysis

Samples from each step of nanocellulose production were subjected to thermogravimetric analysis in order to test their thermal stability. The results are shown in Figure 10, where a little difference between samples can be observed. In all cases, the loss of weight started around $70\text{ }^{\circ}\text{C}$, which was due to evaporation of water, reaching a value close to 5%. After the first stage, the samples suffered the main weight loss at $350\text{ }^{\circ}\text{C}$, where around 70-75% of the material was degraded. On the other hand, the nanocellulose samples showed a slightly higher loss of water than the pulp samples, reaching values of 10%. Moreover, the main weight loss occurred at about $210\text{--}220\text{ }^{\circ}\text{C}$ (T_{onset}), for the samples resulting from 3 and 5 homogenizer passes, reaching a maximum value of 55% and 45%, respectively. Up to this temperature, the weight loss drops in a moderate way, reaching values of 75 and 65%, for the 3 homogenizer-passes sample and the 5 homogenizer-passes sample, respectively. The results seem to reveal that the nanocellulose film was less stable against temperature than the organosolv and bleached pulps, and this can be attributed to the sodium carboxylate groups formed in basic TEMPO-oxidation.²⁷

On the other hand, the differential thermal curves (Fig. 10 inset image) show that, while the pulps present only one peak, the thermal degradation of the nanocellulose was reflected in two peaks: the

smaller one – at about $230\text{--}240\text{ }^{\circ}\text{C}$ – can be attributed to carboxylates groups,²⁸ and the second one can be attributed to cellulose degradation. The latter appeared at a lower temperature than the peak for the pulps, and the different particle size can be the reason for this shift of temperature. In conclusion, both thermal profile figures show the effect of TEMPO-oxidation on the fibres.

XRD analysis

Figure 11 shows the XRD patterns of organosolv pulp (F1), bleached pulp (FEPAB) and of the nanocelluloses obtained after 3 and 5 homogenizer passes (Film 03 and Film 05). In the patterns, the three main peaks corresponding to cellulose I can be observed, namely: at 16° , 23° and 34° for (110), (200) and (004) reflection planes, respectively.²⁹ From the application of Segal's equation,¹⁸ the crystallinity index was calculated, and the results are listed in Table 8. The results show an increase in crystallinity, which can be explained by the degradation of the amorphous region of cellulose when the samples underwent heat and chemical treatments. The highest degree of crystallinity corresponded to the bleached pulp (87.9%), which was higher than that reported by Lu *et al.*³⁰ for the pine wood treated with dilute sulfuric acid (64.2%). However, when the cellulose pulp was subjected to TEMPO-oxidation at high pH, crystalline region of cellulose started degrading too, which resulted in

lower crystallinity index, registering around 81%. This value is consistent with that reported by Barbash *et al.*,³¹ when they treated organosolv pulp from reed stalks with TEMPO reagent. They reported that the crystallinity index decreased as the time of operation increased. Other cases have been reported in scientific literature by Sánchez *et al.*,³² who treated different wheat straw pulps, and Tang *et*

al.,³³ who treated bamboo dissolving pulp. Meanwhile, the homogenization process, as any mechanical treatment, contributed to the destruction of crystalline cellulose. Thus, Lu *et al.*³⁴ observed the same effect when bamboo chips were extruded twice in a screw extrusion device.

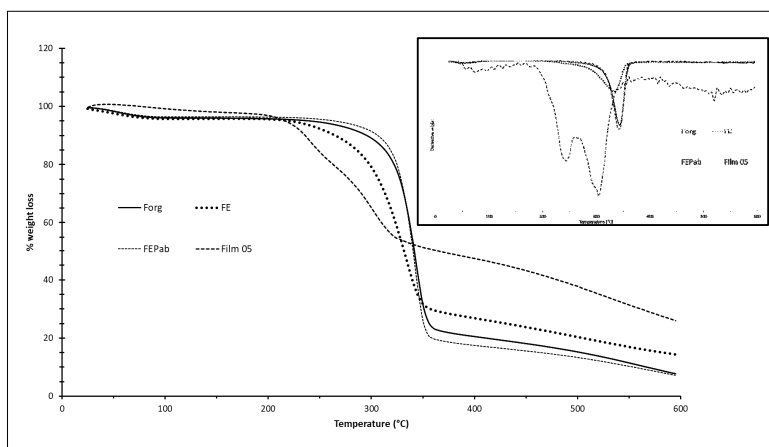


Figure 10: Thermogravimetry analysis of organosolv pulp (Forg), pulp after alkaline process (FE), bleached pulp (FEPab) and nanocellulose obtained after 5 homogenizer passes (Film 05)

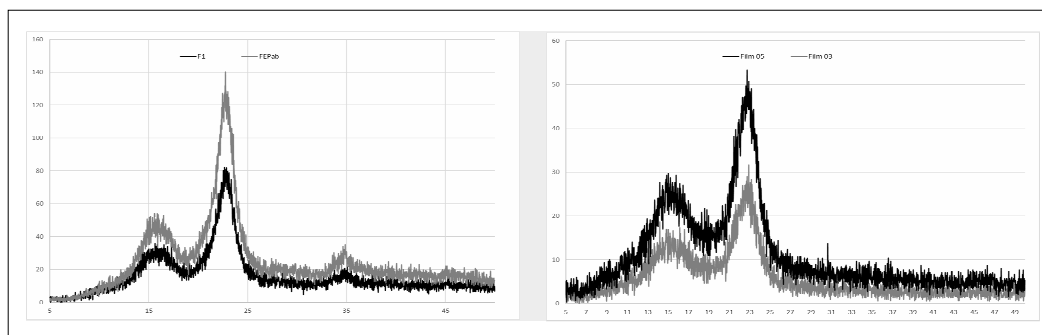


Figure 11: X-ray diffraction patterns of organosolv pulp (F1), bleached pulp (FEPab), and nanocellulose obtained after 3 and 5 homogenizer passes (Films 03 and 05)

Table 8
Crystallinity index of treated samples

Sample	CI (%)
Organosolv pulp (F1)	83.7
Pulp after alkaline bleaching (FE)	83.8
Bleached pulp (FEPab)	87.9
5 homogenizer-passes nanocellulose	72.8

CONCLUSION

Pine wood was used to obtain nano-size fibres by mechanical fibrillation after TEMPO-oxidation. First, a two-step performic acid process was

investigated and optimized following EPab bleaching to remove the lignin and hemicelluloses. This system produced highly pure bleached pulp, with a low kappa index of 2, hardly losing any

material. These samples were subjected to TEMPO-oxidation under different conditions, and the results of the optimized treatment showed a value of 9 mmol COOH/g fibre. Finally, oxidized fibres were homogenized at different pressure levels and with different numbers of passes through the homogenizer. It was found that neither the number of homogenizer passes, nor pressure affected the diameter of the fibrils.

REFERENCES

- ¹ R. Kamel, N. A. El-Wakil, A. Dufresne and N. A. Elkasabgy, *Int. J. Biol. Macromol.*, **163**, 1579 (2020), <https://doi.org/10.1016/j.ijbiomac.2020.07.242>
- ² D. Theng, G. Arbat, M. Delgado-Aguilar, F. Vilaseca, B. Ngo *et al.*, *Ind. Crop. Prod.*, **75**, 166 (2015), <https://doi.org/10.1016/j.indcrop.2015.06.046>
- ³ Z.-Y. Qin, G.-L. Tong, Y. C. F. Chin and J.-C. Zhou, *BioResources*, **6**, 1136 (2011), <https://doi.org/10.15376/biores.6.2>
- ⁴ A. Chaker, P. Mutjé and M. Rei, *Cellulose*, **21**, 4247 (2014), <https://doi.org/10.1007/s10570-014-0454-5>
- ⁵ S. Abad, V. Santos and J. C. Parajó, *J. Wood Chem. Technol.*, **19**, 225 (1999), <https://doi.org/10.1080/02773819909349610>
- ⁶ F. Cebreiros, L. Clavijo, E. Boix, M. D. Ferrari and C. Lareo, *Renew. Energ.*, **149**, 115 (2020), <https://doi.org/10.1016/j.renene.2019.12.024>
- ⁷ H. Li, X. Cai, Z. Wang and C. Xu, *J. Supercrit. Fluids*, **158**, 104745 (2020), <https://doi.org/10.1016/j.supflu.2019.104745>
- ⁸ P. Ligeró, J. J. Villaverde, A. Vega and M. Bao, *Ind. Crop. Prod.*, **27**, 110 (2008), <https://doi.org/10.1016/j.indcrop.2007.08.008>
- ⁹ A. Vega and P. Ligeró, *Ind. Crop. Prod.*, **97**, 252 (2017), <https://doi.org/10.1016/j.indcrop.2016.12.02>
- ¹⁰ A. Seisto and K. Poppius, in *Procs. 8th International Symposium on Wood and Pulping Chemistry*, June 6–9, 1995, Helsinki, Finland, vol. 1, pp. 407–414
- ¹¹ A. Seisto and K. Poppius, *Tappi J.*, **80**, 215 (1997), <https://imrise.tappi.org/TAPPIProducts/97/SEP/97SE/P215.aspx>
- ¹² K. Dimos, T. Paschos, A. Louloudi, K. G. Kalogiannis, A. A. Lappas *et al.*, *Fermentation*, **5**, 5 (2019), <https://doi.org/10.3390/fermentation5010005>
- ¹³ P. Ligeró, J. J. Villaverde, A. Vega and M. Bao, *Bioresour. Technol.*, **99**, 5687 (2008), <https://doi.org/10.1016/j.biortech.2007.10.028>
- ¹⁴ D. Watkins, Md. Nuruddin, M. Hosur, A. Tcherbi-Narteh and S. J. Jeelani, *Mater. Res. Technol.*, **4**, 26 (2015), <https://doi.org/10.1016/j.jmrt.2014.10.009>
- ¹⁵ M.-F. Li, S.-N. Sun, F. Xu and R.-C. Sun, *Chem. Eng. J.*, **179**, 80 (2012), <https://doi.org/10.1016/j.cej.2011.10.060>
- ¹⁶ S. Abad, V. Santos and J. C. Parajó, *Holzforschung*, **54**, 544 (2000), <https://doi.org/10.1515/HF.2000.092>
- ¹⁷ S. Bauer and A. B. Ibañez, *Biotechnol. Bioeng.*, **111**, 11 (2014), <https://doi.org/10.1002/bit.25276>
- ¹⁸ L. Segal, J. J. Creely, A. E. Martin and C. M. Conrad, *Text. Res. J.*, **29**, 786 (1959), <https://doi.org/10.1177/004051755902901>
- ¹⁹ J. J. Villaverde, P. Ligeró and A. Vega, *Ind. Eng. Chem. Res.*, **48**, 9830 (2009), <https://doi.org/10.1021/ie9008277>
- ²⁰ B. D. Mattos, T. V. Lourençon, D. C. Gatto, L. Serrano and J. Labidi, *Wood Mater. Sci. Eng.*, **11**, 209 (2016), <https://doi.org/10.1080/17480272.2014.970574>
- ²¹ N. Cruz, C. Bustos, M. G. Aguayo, A. Cloutier and R. Castillo, *Bioresources*, **13**, 2268 (2018), <https://doi.org/10.15376/biores.13.2.2268-2282>
- ²² S. Matsuki, H. Kayano, J. Takada, H. Kono, S. Fujisawa *et al.*, *ACS Sustain. Chem. Eng.*, **8**, 17800 (2020), <https://doi.org/10.1021/acsschemeng.0c06515>
- ²³ A. Serra, I. González, H. Olivier-Ortega, Q. Tarrés, M. Delgado-Aguilar *et al.*, *Polymers*, **9**, 557 (2017), <https://doi.org/10.3390/polym9110557>
- ²⁴ I. Besbes, S. Alila and S. Boufi, *Carbohydr. Polym.*, **84**, 975 (2011), <https://doi.org/10.1016/j.carbpol.2010.12.052>
- ²⁵ E. Robles, J. Fernández-Rodríguez, A. M. Barbosa, O. Gordobil, N. L. V. Carreó *et al.*, *Carbohydr. Polym.*, **183**, 294 (2018), <https://doi.org/10.1016/j.carbpol.2018.01.015>
- ²⁶ S. Fujisawa, Y. Okita, H. Fukuzumi, T. Saito and A. Isogai, *Carbohydr. Polym.*, **84**, 579 (2011), <https://doi.org/10.1016/j.carbpol.2010.12.029>
- ²⁷ H. Fukuzumi, T. Saito, T. Iwata, Y. Kumamoto and A. Isogai, *Biomacromolecules*, **10**, 162 (2008), <https://doi.org/10.1021/bm801065u>
- ²⁸ X. Sun, Q. Wu, S. Ren and T. Lei, *Cellulose*, **22**, 1123 (2015), <https://doi.org/10.1007/s10570-015-0574-6>
- ²⁹ A. D. French, *Cellulose*, **21**, 885 (2014), <https://doi.org/10.1007/s10570-013-0030-4>
- ³⁰ H. Lu, L. Zhang, M. Yan, K. Wang and J. Jiang, *Carbohydr. Polym.*, **277**, 1 (2022), <https://doi.org/10.1016/j.carbpol.2021.118897>
- ³¹ V. A. Barbash, O. V. Yashchenko, A. S. Gondovska and I. M. Deykun, *Appl. Nanosci.*, **12**, 835 (2022), <https://doi.org/10.1007/s13204-021-01749-z>
- ³² R. Sánchez, E. Espinosa, J. Domínguez-Robles, J. M. Loaiza and A. Rodríguez, *Int. J. Biol. Macromol.*, **92**, 1025 (2016), <https://doi.org/10.1016/j.ijbiomac.2016.08.019>
- ³³ Z. Tang, W. Li, X. Lin, H. Xiao, Q. Miao *et al.*, *Polymers*, **9**, 421 (2017), <https://doi.org/10.3390/polym9090421>
- ³⁴ H. Lu, L. Zhang, C. Liu, Z. He, X. Zhou *et al.*, *Cellulose*, **25**, 7043 (2018), <https://doi.org/10.1007/s10570-018-2067-x>